

## Specific fluorescent detection of fibrillar $\alpha$ -synuclein using mono- and trimethine cyanine dyes

K. D. Volkova,<sup>a</sup> V. B. Kovalska,<sup>a</sup> A. O. Balanda,<sup>a</sup> M. Yu Losytskyy,<sup>a</sup> A. G. Golub,<sup>a</sup>  
R. J. Vermeij,<sup>b</sup> V. Subramaniam,<sup>b</sup> O. I. Tolmachev<sup>c</sup> and S. M. Yarmoluk<sup>a,\*</sup>

<sup>a</sup>*Institute of Molecular Biology and Genetics, NASU, 150 Zabolotnogo Street, 03143 Kyiv, Ukraine*

<sup>b</sup>*MESA+ Institute for Nanotechnology, Biophysical Engineering Group, University of Twente, The Netherlands*

<sup>c</sup>*Institute of Organic Chemistry, National Academy of Sciences of Ukraine, Murmans'ka Str. 5, 02094 Kyiv, Ukraine*

Received 14 May 2007; revised 3 October 2007; accepted 17 October 2007

Available online 22 October 2007

**Abstract**—With the aim of searching of novel amyloid-specific fluorescent probes the ability of series of mono- and trimethine cyanines based on benzothiazole, pyridine and quinoline heterocycle end groups to recognize fibrillar formations of  $\alpha$ -synuclein (ASN) was studied. For the first time it was revealed that monomethine cyanines can specifically increase their fluorescence in aggregated ASN presence. Dialkylamino-substituted monomethine cyanine T-284 and meso-ethyl-substituted trimethine cyanine SH-516 demonstrated the higher emission intensity and selectivity to aggregated ASN than classic amyloid stain Thioflavin T, and could be proposed as novel efficient fluorescent probes for fibrillar ASN detection. Studies of structure–function dependences have shown that incorporation of amino- or diethylamino- substituents into the 6 position of the benzothiazole heterocycle yields in a appearance of a selective fluorescent response to fibrillar  $\alpha$ -synuclein presence. Performed calculations of molecular dimensions of studied cyanine dyes gave us the possibility to presume, that dyes bind with their long axes parallel to the fibril axis via insertion into the neat rows (so called ‘channels’) running along fibril.

© 2007 Elsevier Ltd. All rights reserved.

### 1. Introduction

Amyloid aggregates are hallmarks of neurodegenerative diseases, such as Alzheimer's, Parkinson's, and Huntington's disease, and of the prion diseases. Parkinson's disease (PD) is the second most common neurodegenerative disease affecting about 1–2% of the population over the age of 65.<sup>1</sup> The human  $\alpha$ -synuclein protein plays a central role in the etiology of Parkinson's disease,<sup>2</sup> and forms fibrillar aggregates that are found in Lewy bodies in the brain, structures which are characteristic of the disease.<sup>3–5</sup>

Detection of ASN and other amyloid fibrils is usually performed by measuring the strongly enhanced fluorescence emission of specific fluorescent probes upon interaction with amyloid fibrils. The benzothiazole dye Thioflavin T<sup>6,7</sup> and the symmetrical sulfonated azo dye Congo Red<sup>8</sup> and its derivatives<sup>9</sup> are most commonly used.

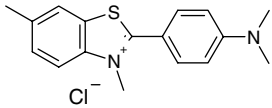
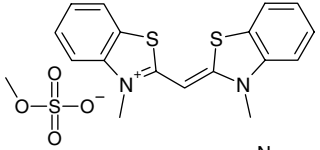
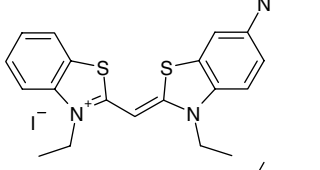
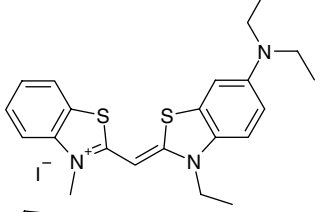
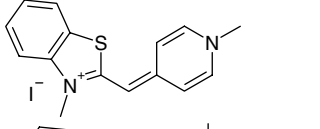
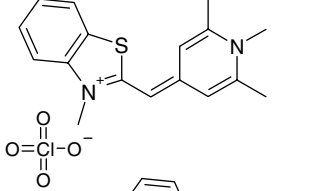
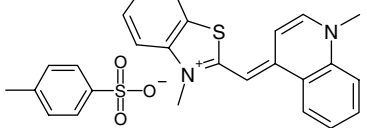
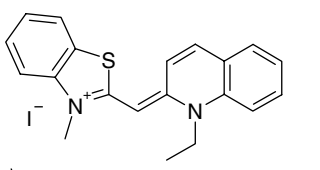
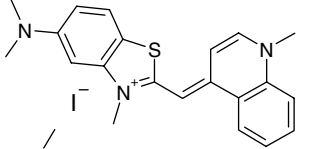
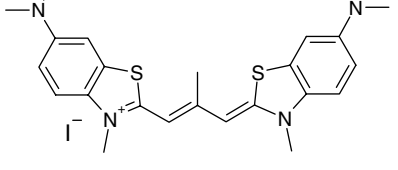
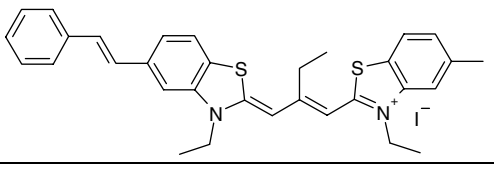
However existing fibril detection assays have revealed several drawbacks. Thioflavin T is not always a quantitative predictor of degree of fibrillization because its fluorescence can vary depending on the structure and morphology of the fibrils.<sup>10</sup> Congo Red was shown to bind also to native  $\alpha$ -helical proteins such as citrate synthase and interleukin-2.<sup>11</sup> Other drawbacks include a great variability among the different amyloids in the binding of Thioflavin T and Congo Red. Thus the design of new dyes which can selectively interact with fibrillar amyloidogenic proteins is of substantial importance for basic research, and has a practical significance for biotechnology and medicine.

We have proposed trimethine cyanine dyes as specific fluorescent probes for aggregated protein structures.<sup>12</sup> The meso-substituted symmetric cyanine T-49 (Table 1) with amino substituents in the benzothiazole heterocycle demonstrated a significant fluorescence intensity increase upon interaction with fibrillar  $\beta$ -lactoglobulin (BLG) and showed a relatively weak response in the presence of native protein. The increase in emission intensity in the presence of aggregated BLG of the meso-substituted asymmetric dye SH-516 (Table 1), con-

**Keywords:** Cyanine dyes;  $\alpha$ -Synuclein; Fluorescent detection.

\* Corresponding author. Tel./fax: +380 44 522 24 58; e-mail: [sergiy@yarmoluk.org.ua](mailto:sergiy@yarmoluk.org.ua)

**Table 1.** Structures and molecular dimensions of dyes studied

Dye	Structure	x-, y-, and z-principal axes lengths (Å)
Thioflavin T		x = 14.24 y = 5.40 z = 3.64
L-43		x = 13.58 y = 6.45 z = 2.06
T-414		x = 13.95 y = 8.21 z = 2.70
T-284		x = 16.26 y = 9.29 z = 4.49
PO		x = 12.9 y = 6.13 z = 2.03
Cyan-40		x = 12.97 y = 6.37 z = 1.84
TO		x = 13.12 y = 7.21 z = 1.83
SH-395		x = 13.91 y = 7.24 z = 3.26
T-196		x = 15.38 y = 7.04 z = 1.83
T-49		x = 20.18 y = 7.34 z = 1.98
SH-516		x = 23.14 y = 8.55 z = 3.27

taining a styryl fragment in the benzothiazole heterocycle, was up to 5 times higher than the increase of Thioflavin T fluorescence. We have used fluorescence spectroscopy to explore the ability of the trimethine cyanines and a series of monomethine cyanines based on benzothiazole, pyridine, and quinoline heterocycle end groups (Table 1) to selectively recognize fibrillar ASN.

To gain insight into dye/aggregated protein complex formation, we have performed calculations of molecular dimensions (namely of the *x*-, *y*-, and *z*-principal axes lengths) of the mono- and trimethine cyanine dyes (Fig. 1) studied. These data could help to estimate the correlation between the size and thus nature of the molecule and its ability to selectively interact with fibrillar ASN. Determination of the structural drivers of dye binding to amyloid fibrils has received significant attention, because elucidation of this mechanism has not only crucial importance for the development of novel highly fluorescent amyloid-specific probes but could also give us insight into the aggregation process.<sup>13–15</sup>

A general model for amyloid-specific dye binding to amyloid fibrils was proposed by Krebs et al. on the basis of Thioflavin T. Confocal microscopy studies using polarized light and Thioflavin T molecular dimension calculations revealed that the dye binds to the fibrils with its long axis parallel to the fibril axis via insertion into the ‘binding channel’ running along the fibril. The width of such ‘binding channels’ is the distance between every second residue, which in an average  $\beta$ -sheet is 6.5–

6.95 Å. Thus to ensure a sterically favourable fit into the channel, the dye molecular dimension should not exceed the width of ‘binding channel’.<sup>16</sup>

Finally we have calculated binding constants ( $K_b$ ) for the dye–fibril complexes for the most promising dyes.

## 2. Results and discussion

### 2.1. Spectral properties of dyes in buffer and in the presence of monomeric ASN

Fluorescence properties of the free monomethine and trimethine cyanine dyes (Table 1) in buffer are presented in Table 2. We use the commonly used commercially available benzothiazole dye Thioflavin T as a reference dye.<sup>7,16</sup>

Excitation spectra maxima for monomethine cyanines lie in the range of 400–520 nm. For trimethine cyanines T-49 and SH-516 these maxima are located at 575 and 562 nm, respectively. For Thioflavin T the excitation maximum is situated at 339 nm. Maximum wavelengths of the fluorescence emission spectra for the mono- and trimethine cyanine dyes studied here lie between 470 and 698 nm. For Thioflavin T the emission spectrum maximum is situated at 442 nm (Table 2). All of the dyes studied exhibit low intrinsic fluorescence intensities ( $I_0$ ) between 0.6 and 17 a.u.

The majority of the mono- and trimethine cyanine dyes considered demonstrate large Stokes shift values (60–207 nm). The noticeable Stokes shift value for L-43 (80 nm) is probably caused by aggregation of dye in aqueous solution (data not shown). Intramolecular charge transfer caused by the presence of the dialkylamino groups in the heterocycle could be the reason for the large Stokes shift values (137 and 207 nm, respectively) observed for monomethines T-284 and T-196 as well as for the trimethine cyanine T-49 (60 nm).<sup>17</sup> The same process possibly occurs in the case of the symmetrical monomethine cyanine T-414, containing an amino group in the benzothiazole heterocycle, leading to a comparatively large (83 nm) observed Stokes shift. For unsymmetrical monomethines PO, Cyan-40, and TO, moderate Stokes shift values are observed (25–30 nm). For the meso-ethyl-substituted trimethine cyanine dye SH-516 the observed Stokes shift is small (6 nm).

Fluorescence properties of the dyes studied in the presence of monomeric ASN are shown in Table 2. For most of the mono- and trimethine cyanines, and for Thioflavin T, the positions of excitation and emission maxima stay unchanged or shift insignificantly compared with those for the free dye in buffer. The only exceptions are the monomethine cyanines T-414 and T-284, for which a short-wavelength shift of fluorescence spectra maxima positions in 4 and 7 nm, respectively, is observed. The observed Stokes shifts for the dyes in the presence of monomeric ASN remained similar to those of free dyes in buffer. A majority of the cyanine dyes studied showed little or no increase in fluorescence

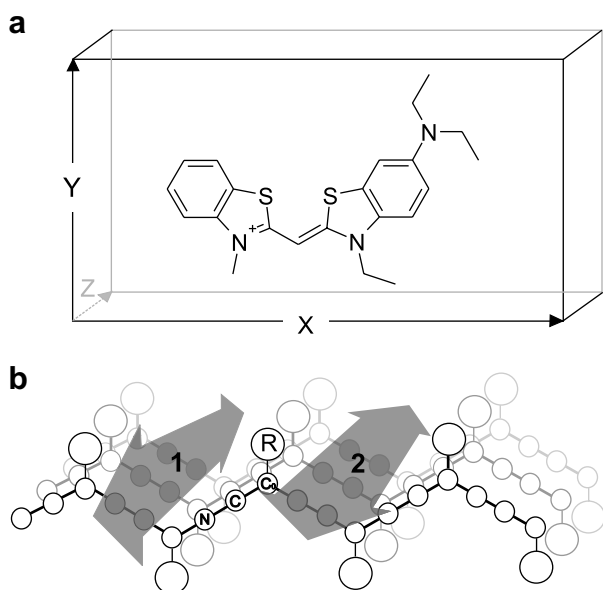


**Figure 1.** (a) Schematic representation of the *x*-, *y*-, and *z*-principal axes of the monomethine T-248. (b) Schematic representation of a  $\beta$ -sheet and possible position of dye molecules (gray arrows) in the ‘binding channel’ based on work of Krebs et al.<sup>16</sup> Arrow 1 represents dye interaction with the fibril via Binding Mode 1, arrow 2—via Binding Mode 2. The backbone atoms (N, C, and C<sub>O</sub>) and the side chain (R) for one residue are indicated. No hydrogen bonds are indicated. This scheme is valid for both parallel and anti-parallel sheets. If part of a fibril, the long axis of the fibrils would be perpendicular to the surface of this page.<sup>18</sup>

**Table 2.** Spectral properties of the dyes freely dissolved in buffer and in the presence of monomeric and fibrillar ASN

Dye	In free form			In the presence of monomeric ASN				In the presence of fibrillar ASN			
	$\lambda_{\text{ex}}$ (nm)	$\lambda_{\text{em}}$ (nm)	$I_0$ (a.u.)	$\lambda_{\text{ex}}$ (nm)	$\lambda_{\text{em}}$ (nm)	$I^{\text{ASN}}[\text{N}]$ (a.u.)	$\lambda_{\text{ex}}$ (nm)	$\lambda_{\text{em}}$ (nm)	$I^{\text{ASN}}[\text{F}]$ (a.u.)	$I^{\text{ASN}}[\text{F}]/I_0$	$I^{\text{ASN}}[\text{F}]/I^{\text{ASN}}[\text{N}]$
L-43	400	481	17	400	481	12.4	429	470	20.4	1.2	1.65
T-414	437	520	3.2	437	516	3.3	444	526	11.3	3.53	3.4
T-284	443	580	2.86	443	573	2.2	441	570	21	7.34	9.55
PO	455	481	2.1	455	481	3.6	455	481	8	3.8	2.22
Cyan-40	440	470	7.35	437	471	9.2	451	485	41.1	5.6	4.5
TO	505	530	1.16	505	530	1.9	505	530	1.9	1.63	1
SH-395	470	560	0.6	470	560	0.9	470	555	3.3	5.5	3.67
T-196	491	698	0.49	491	698	0.46	491	698	0.46	0.94	1
T-49	575	635	1.4	575	635	0.82	575	635	1	0.7	1.22
SH-516	562	568	2.3	562	572	2.77	570	580	20.5	8.9	7.4
Thio-T	339	442	1.79	339	442	2.1	440	478	6.1	3.4	2.9

$\lambda_{\text{ex}}$  ( $\lambda_{\text{em}}$ )—maximum wavelength of fluorescence excitation (fluorescence emission) spectrum.

$I_0$ —fluorescence intensity of free dye in buffer.

$I^{\text{ASN}}[\text{N}]/(I^{\text{ASN}}[\text{F}])$ —emission intensity of dye in presence of monomeric (fibrillar) ASN.

intensity, while a select few exhibited a decrease in emission intensity in the presence of monomeric ASN (Table 2).

## 2.2. Spectral properties of dyes in the presence of fibrillar ASN

Fluorescence characteristics of the mono- and trimethine cyanines in the presence of fibrillar ASN are described in Table 2. The excitation maxima positions of most of the dyes remain almost unchanged in the presence of fibrillar ASN relative to those in aqueous buffer. A bathochromic shift of excitation maxima of 8–11 nm is observed only for T-414, Cyan-40, and SH-516.

Similar to the results obtained with monomeric protein, addition of fibrillar ASN only slightly influences the emission maxima position for almost all studied mono- and trimethine cyanines relative to those in aqueous buffer. For the symmetrical monomethine T-284, the emission maximum position is blue-shifted by 10 nm upon the addition of fibrillar ASN. For dyes T-414, Cyan-40, and SH-516 long-wavelength shifts of 6–15 nm were noticed. The observed values of Stokes shifts are in the same range as for the dyes in the presence of monomeric ASN. For Thioflavin T, characteristic bathochromic shifts of the emission and excitation maxima positions by 101 and 36 nm, respectively, were observed.

For most of the dyes fluorescence intensity increases ( $I^{\text{ASN}}[\text{F}]/I_0$ ) of a factor of 1.6–8.9 were noticed in the presence of fibrillar ASN (Table 2). The exceptions are the 6,6'-dimethylamino substituted trimethine cyanine dye T-49 and the unsymmetrical monomethine cyanine T-196, which lost their fluorescence in the presence of fibrillar ASN ( $I^{\text{ASN}}[\text{F}]/I_0$  values  $\sim 0.7$  and 0.9, respectively). The same concentration of fibrillar ASN ( $10^{-6}$  M) yields an emission intensity increase of 2.9 times for Thioflavin T, while at higher protein concentration ( $2.5 \times 10^{-6}$  M) the emission of dye was enhanced up to 6 times. The values of emission increase obtained for Thioflavin T are in correspondence with the literature data.

To compare dye binding specificity for fibrillar ASN, we compared the values of fluorescence intensity observed for each dye in the presence of fibrillar ASN ( $I^{\text{ASN}}[\text{F}]$ ) with those in the presence of monomeric ASN ( $I^{\text{ASN}}[\text{N}]$ ) (Table 2).

The highest  $I^{\text{ASN}}[\text{F}]/I^{\text{ASN}}[\text{N}]$  value ( $\sim 9.5$ ) was observed for the dialkylamino-substituted monomethine cyanine T-284 (Fig. 2), which is 3 times higher than for Thioflavin T ( $\sim 2.9$ ). The amino-substituted monomethine T-414 also demonstrated comparatively high binding preference to fibrillar ASN ( $\sim 3.4$ ), while for unsubstituted dye L-43 this value was rather low ( $\sim 1.6$ ). Thus dye T-284 is considered to be a potential fluorescent probe for selective detection of fibrillar ASN.

For the unsymmetrical monomethines with 4-(pyridine) (PO), 4-(dimethylpyridine) (Cyan-40), and 2-(quinoline) (SH-395) heterocycle,  $I^{\text{ASN}}[\text{F}]/I^{\text{ASN}}[\text{N}]$  values were comparable to or exceeded those for Thioflavin T. TO and T-196 monomethines with 4-(quinoline) heterocycle as well as the trimethine cyanine T-49 showed weak fluo-

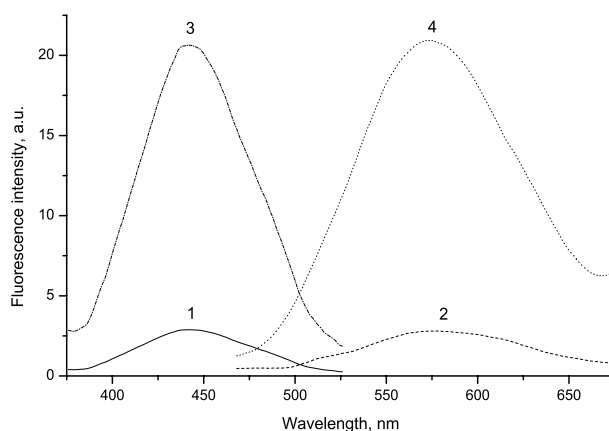


**Figure 2.** Fluorescence excitation (left) and emission (right) spectra of the monomethine cyanine dye T-284 ( $5 \times 10^{-6}$  M) in the presence of  $10^{-6}$  M monomeric ASN (1 and 2, respectively) and fibrillar ASN (3 and 4, respectively).

rescence responses in the presence of both monomeric and fibrillar protein.

Among the trimethine cyanine dyes studied, meso-ethyl-substituted trimethine cyanine SH-516 showed a high  $I^{\text{ASN}}[\text{F}]/I^{\text{ASN}}[\text{N}]$  value, more than twice that for Thioflavin T (7.6 and 2.9, respectively). SH-516 was previously found by us to give a strong fluorescent response in the presence of fibrillar  $\beta$ -lactoglobulin (BLG),<sup>12</sup> and is thus a potential candidate for the specific detection of fibrillar amyloid-like aggregates.

### 2.3. Cyanine dyes/fibrillar ASN binding mode studies

Despite the lack of detailed understanding of the mechanism of dye interaction with amyloid fibrils, most of the binding models state that amyloid-specific dyes such as Thioflavin T and Congo Red bind with their long axis parallel to the fibril axis.<sup>18,19</sup> It has been reported that side chains on each side of the  $\beta$ -sheet form neat rows (so-called ‘channels’) running along the fibril and therefore perpendicular to the strands.<sup>20,21</sup> The width of such ‘binding channels’ is the distance between every second residue, which is 6.5–6.95 Å in an average  $\beta$ -sheet. However, the free space in these channels is likely to be still less, since the mentioned values do not take into account the volume occupied by the side chains.<sup>21</sup> Krebs et al. studied binding of Thioflavin T to amyloid fibrils and based on this dye’s molecular dimensions (15.2 Å; 6.1 Å; 4.3 Å) what are these values ( $x, y, z$ ) suggested that the dye most likely inserts itself into these binding channels with its shortest axis perpendicular to the fibril axis (Fig. 1).<sup>16</sup> The close proximity of the side chains to the dyes when bound to the amyloid fibrils is likely to result in steric interactions between them. Such interactions lead to immobilization of the dye molecule in the channel and further restrict intramolecular dye torsion (rotation), which results in fluorescence intensity enhancement.

To get insight into dye/fibrillar ASN complex formation, we have calculated the molecular dimensions ( $x$ -,  $y$ -, and  $z$ -principal axes lengths) of the studied mono- and trimethine cyanine dyes (Table 1). We assumed that for effective interaction with the ‘binding channel’, the molecular dimensions of the dye molecule along either  $y$ - or  $z$ -axis (or both) should not exceed 6.5 Å (the supposed width of ‘binding channel’).

The majority of the dyes considered in this report (with the exception of the symmetrical monomethine L-43 and the unsymmetrical dyes PO and Cyan-40) have molecular dimensions along the  $y$ -axis which exceed the width of the fibril ‘binding channel’ (from 7.04 to 9.29 Å). Thus incorporation of these dyes into the channel with their  $z$ -axes parallel to the fibril axis is likely to be unfavourable. Thus, the most likely mode of binding for these dyes is with the  $z$ -axis perpendicular to the fibril axis (Binding Mode 1) (Fig. 1(B1)).

Although Cyan-40 and PO dyes seem to be too thin along the  $z$ -axis (up to 2.03 Å) to fit into the ‘binding channel’, these dyes specifically increase their fluores-

cence in the presence of fibrillar ASN. However, the molecular dimensions of these dyes along their  $y$ -principal axes are 6.13 and 6.37 Å, respectively, which potentially allows these dye molecules to fit in the fibril’s ‘binding channel’ with their  $z$ -axes parallel to the fibril axis (Binding Mode 2) (Fig. 1(B2)).

Monomethines T-414, T-284, SH-395, as well as the trimethine cyanine SH-516, which demonstrated high binding preference to aggregated ASN values ( $I^{\text{ASN}}[\text{F}]/I^{\text{ASN}}[\text{N}] \sim 3.4\text{--}9.5$ ) have molecular dimensions along their  $z$ -axes ranging from 2.7 to 4.49 Å and thus could fit in the binding channel by Binding Mode 1.

The unsymmetrical monomethine cyanines TO and T-196 containing a 4-(quinoline) heterocycle and symmetrical trimethine T-49 show little, if any, enhancement of fluorescence in the presence of monomeric or fibrillar ASN. These dyes are only up to 1.93 Å long along their  $z$ -axes, which seems insufficient to fit into the channel. Despite the fact that the dimension of the symmetrical monomethine L-43 along its  $y$ -axis is 6.45 Å, which potentially allows a fit into the fibril channel, this dye demonstrated low binding selectivity to fibrillar ASN.

It could be hypothesized that dyes with a bulky heterocyclic system fit more snugly in the fibril channel than smaller dyes. However this criterion is limited by a critical molecule size, since molecules that are too large lose their capability to enter and fit into the fibril ‘binding channel’ due to steric hindrance. Our study suggests that dye molecules with favorable molecular dimensions (about 3 Å along  $z$ -axis and up to 6.5 Å along  $y$ -axis) could preferentially insert into ‘binding channels’ with their  $z$ -axes parallel or perpendicular to the fibril axis, closely surrounded by the protein side chains.

### 2.4. Binding constant estimation for selected dye/protein complexes

We performed fluorescent titrations of increasing amounts of the most promising dyes, 6-diethylamino-substituted monomethine cyanine T-284 and meso-ethyl-substituted trimethine cyanine SH-516, in the presence of 0.5  $\mu\text{M}$  of ASN fibrils. Equilibrium constants of dye binding to the ASN fibrils ( $K_b$ ) were estimated (Figs. 3 and 4) from these data.

Dissociation constants ( $K_d$ ) of Thioflavin T and aggregated species of synthetic peptides p(1–28) and p(1–40) whose sequences are derived from a protein ( $\beta\text{A4}$ ) isolated from deposits found in the brains of patients with Alzheimer’s disease<sup>22</sup> have been reported.<sup>7</sup> Taking into account that  $K_b = 1/K_d$ , the results reported in Ref. 7 indicate that Thioflavin T binding to peptide p(1–40) is of lower affinity ( $K_b = 0.5 \times 10^6 \text{ M}^{-1}$ ) than for dye/p(1–28) complex  $K_b = 1.85 \times 10^6 \text{ M}^{-1}$ .

A double reciprocal plot of the dye–ASN complex fluorescence intensity against the dye concentration (Fig. 4) yields apparent  $K_b$  values at the intercepts with the  $X$ -axis. The same procedure was used for the estimation of the dye–protein complex dissociation constant in



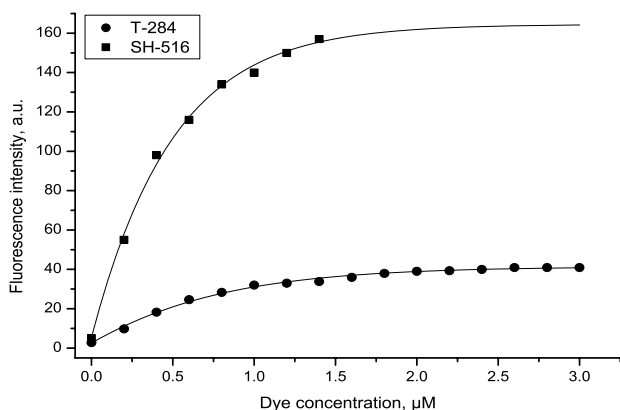


**Figure 3.** Fluorescence titration of 0.5 μM solutions of aggregated ASN with increasing amounts of dyes T-284 and SH-516 in 10 mM Hepes buffer (pH 7.4).

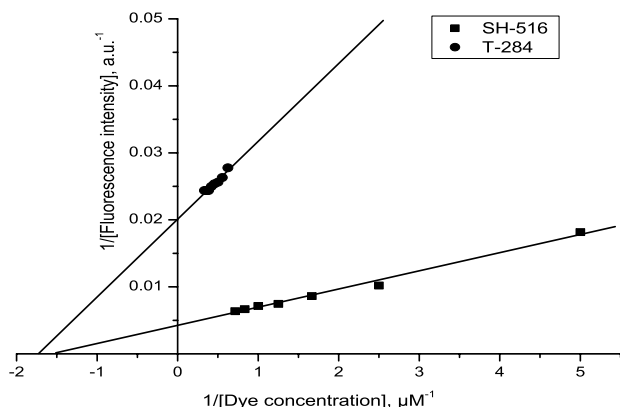


**Figure 4.** Double reciprocal representation of monomethine T-284 ( $K_b = 1.78 \times 10^6 \text{ M}^{-1}$ ) and trimethine cyanine SH-516 ( $K_b = 1.53 \times 10^6 \text{ M}^{-1}$ ) binding to  $\alpha$ -synuclein.

Ref. 7. Our experiments yield  $K_b \sim 1.78 \times 10^6 \text{ M}^{-1}$  for the monomethine cyanine dye T-284 and  $K_b \sim 1.53 \times 10^6 \text{ M}^{-1}$  for the trimethine cyanine SH-516. These  $K_b$  values obtained for the respective dye/ASN fibril complexes are comparable with the corresponding values for Thioflavin T binding with aggregated synthetic peptides.

### 3. Conclusions

1. A series of monomethine and trimethine cyanines based on benzothiazole, pyridine and quinoline heterocycle end groups were characterized by fluorescence spectroscopy as potential fluorescent probes for selective detection of fibrillar ASN. At the concentrations of fibrillar ASN used, six of ten dyes studied (T-414, T-284, PO, Cyan-40, SH-395, and SH-516) demonstrated comparable or higher emission intensity enhancements than the classic amyloid stain Thioflavin T. Thus cyanines are proposed as a promising class of fluorescent molecules for development of stains sensitive to aggregated proteins.

2. The presence of amino- (dye T-414) or diethylamino- (dye T-284) substituents in the 6 position of the benzothiazole heterocycle yields a selective fluorescent response to fibrillar  $\alpha$ -synuclein in contrast to the corresponding unsubstituted dye.
3. Based on the literature data<sup>16</sup> and by comparing data of fluorescent studies and molecular dimension calculations, we suggest that dyes having favorable molecular dimensions (about 3 Å along z-axis and up to 6.5 Å along y-axis) could insert into 'binding channels' with z-axes parallel or perpendicular to the fibril axis, closely surrounded by the side chains.
4. The largest increases in emission intensity in the presence of fibrillar ASN compared to monomeric protein ( $I^{\text{ASN}}[\text{F}]/I^{\text{ASN}}[\text{N}]$ ) were observed for the dialkylamino-substituted monomethine cyanine T-284 ( $\sim 9.5$  times), and meso-ethyl-substituted trimethine cyanine SH-516 ( $\sim 7.6$  times). These values are a factor of 2–3 higher than that for Thioflavin T (2.9 times). Absolute emission intensities of these dyes in complexes with fibrillar ASN also exceed that of Thioflavin T. We thus propose the dyes T-284 and SH-516 as novel efficient fluorescent probes for fibrillar ASN detection.
5. For the most efficient dyes, monomethine cyanine T-284 and trimethine cyanine SH-516, fluorescent titrations of increasing amounts of the dyes in the presence of ASN fibrils yielded equilibrium constants of dye binding ( $K_b$ ) to the ASN fibrils. The dyes have similar  $K_b$  values,  $1.78 \times 10^6 \text{ M}^{-1}$  for T-284 and  $1.53 \times 10^6 \text{ M}^{-1}$  for SH-516. These  $K_b$  values are comparable with those reported for Thioflavin T complexed with aggregated synthetic peptides.<sup>3</sup>

## 4. Experimental

### 4.1. Reagents

Ten millimolar Hepes buffer (pH 7.4) containing 50 mM NaCl and 0.02%  $\text{NaN}_3$  was used as solvent. Hepes was purchased from Sigma (St. Louis, USA). Recombinant human ASN was expressed and purified as described.<sup>23</sup>

All monomethine cyanine dyes were synthesized according to Hamer<sup>24</sup>. The T-49 dye was synthesized as described in Ref. 25. The SH-516 dye was kindly provided by Dr. A. Bogolyubskyi (ENAMINE, Kyiv, Ukraine).

### 4.2. Fibrillogenesis of human $\alpha$ -synuclein

Aggregation of wild-type human ASN was performed as described in Ref. 23.

### 4.3. Preparation of stock solutions of dyes and biological molecules

Dye stock solutions ( $2 \times 10^{-3} \text{ M}$ ) were prepared by dissolving the dye in DMSO. The concentrations of proteins in stock solutions were  $10^{-4} \text{ M}$  for both monomeric and fibrillar ASN. The fibrils used in all experiments were from the same batch.

#### 4.4. Preparation of working solutions

Working solutions of free dyes at  $5 \times 10^{-6}$  M were prepared by dilution of the dye stock solution in 10 mM Hepes buffer (pH 7.4). Working solutions of dye–protein complexes were prepared by mixing an aliquot of the dye stock solution (2.5  $\mu$ l) and an aliquot (10  $\mu$ l) of monomeric or fibrillar proteins in 1 ml of buffer. Concentrations of the dye and protein in working solution were  $5 \times 10^{-6}$  M for the dye and  $10^{-6}$  M for both monomeric and aggregated ASN. All working solutions were prepared immediately before the experiment.

#### 4.5. Spectroscopic measurements

Fluorescence excitation and emission spectra were registered on a Cary Eclipse fluorescence spectrophotometer (Varian, Australia). Fluorescence spectra were measured with excitation and emission slit widths set to 5 nm, and at a constant PMT voltage. Spectra were automatically corrected for the wavelength dependence of the excitation source intensity, but were not corrected for the sensitivity of the Cary Eclipse detection system.

Spectroscopic measurements at room temperature were performed in standard quartz cells (1  $\times$  1 cm). All fluorescence emission measurements were made at the respective excitation maxima of each dye.

#### 4.6. Semi-empirical calculations

The AM1 semi-empirical method (HyperChem software) was implemented for geometry optimization in vacuum.<sup>26</sup> The principal parameters of the calculation were: Unrestricted Hartree-Fock,<sup>27</sup> multiplicity 1, convergence limit 0.001. Minimization was performed with conjugate gradient algorithm (Fletcher-Reeves), RMS gradient 0.001 (585 cycles).

#### 4.7. Binding constant estimation

The equilibrium constant  $K_b$  of dye binding to the protein is determined by the general equation:

$$K_b = \frac{C_{bd}}{C_{fd} \times C_{fp}},$$

$C_{bd}$ ,  $C_{fd}$ , and  $C_{fp}$  being the concentrations of the bound dye, free dye, and free protein, respectively. Since the fluorescence intensity of the bound dye exceeds that of the free dye by orders of magnitude, the fluorescence intensity of the dye in the presence of the protein is proportional to  $C_{bd}$ . Considering that  $C_{bd}$  is equal to the concentration of the occupied protein binding sites, the ratio  $C_{bd}/C_{fp}$  may be expressed as  $I/(I_{\max} - I)$ , where  $I$  and  $I_{\max}$  are fluorescence intensities at any given dye concentration and upon reaching saturation, respectively. Since the concentration of dye is in large excess to the protein concentration,  $C_{fd}$  may be approximated as the total dye concentration  $C_d$ , a relationship that is essentially correct upon nearing saturation. Finally, after some transformation, the above equation for  $K_b$  may be expressed as:

$$\frac{1}{I} = \frac{1}{I_{\max}} + \frac{1}{I_{\max}K_b} \times \frac{1}{C_d}$$

Thus, fitting a double reciprocal plot of the dye–protein complex fluorescence intensity dependence on the dye concentration (i.e., the dependence of  $1/I$  on  $1/C_d$ ) by the linear expression  $Y = A + B \times X$  will result in the approximation parameters  $A$  and  $B$ , the ratio  $A/B$  being equal to  $K_b$ . Alternatively, the  $K_b$  value may be obtained as the  $(-1/C_d)$  value of the intercept with the  $X$ -axis. This procedure was used in Ref. 7 for the estimation of the dissociation constant of dye–protein complex.

#### References and notes

- Dusa, A.; Kaylor, J.; Edridge, S.; Bodner, N.; Hong, D.; Fink, A. L. *Biochemistry* **2006**, *45*, 2752.
- Goedert, M. *Nat. Rev. Neurosci.* **2001**, *2*, 492.
- Spillantini, M. G.; Crowther, R. A.; Jakes, R.; Hasegawa, M.; Goedert, M. *Proc. Natl. Acad. Sci. U.S.A.* **1998**, *95*, 6469.
- Spillantini, M. G.; Schmidt, M. L.; Lee, V. M.; Trojanowski, J. Q.; Jakes, R.; Goedert, M. *Nature* **1997**, *388*, 839.
- Shults, C. W. *Proc. Natl. Acad. Sci. U.S.A.* **2006**, *103*, 1661.
- Naiki, H.; Higuchi, K.; Hosokawa, M.; Takeda, T. *Anal. Biochem* **1989**, *177*, 244.
- LeVine, H., 3rd *Protein Sci.* **1993**, *2*, 404.
- Foguel, D.; Suarez, M. C.; Ferrao-Gonzales, A. D.; Porto, T. C.; Palmieri, L.; Einsiedler, C. M.; Andrade, L. R.; Lashuel, H. A.; Lansbury, P. T.; Kelly, J. W.; Silva, J. L. *Proc. Natl. Acad. Sci. U.S.A.* **2003**, *100*, 9831.
- Schmidt, M. L.; Schuck, T.; Sheridan, S.; Kung, M.-P.; Kung, H.; Zhuang, Z.-P.; Bergeron, C.; Lamarche, J. S.; Skovronsky, D.; Giasson, B. I.; Lee, V. M.-Y.; Trojanowski, J. Q. *Am. J. Pathol.* **2001**, *159*, 937.
- Murakami, K.; Irie, K.; Morimoto, A.; Ohigashi, H.; Shindo, M.; Nagao, M.; Shimizu, T.; Shirasawa, T. *J. Biol. Chem.* **2003**, *278*, 46179.
- Khurana, R.; Uversky, V. N.; Nielsen, L.; Fink, A. L. *J. Biol. Chem.* **2001**, *276*, 22715.
- Volkova, K. D.; Kovalska, V. B.; Balanda, A. O.; Vermeij, R. J.; Subramaniam, V.; Slominskii, Yu L.; Yarmoluk, S. M. *J. Biochem. Biophys. Methods*, in press.
- Stopa, B.; Piekarska, B.; Konieczny, L.; Rybarska, J.; Spolnik, P.; Zemanek, G.; Roterman, I.; Krol, M. *Acta Biochim. Pol.* **2003**, *50*, 1213.
- Westermarck, G. T.; Johnson, K. H.; Westermarck, P. *Methods Enzymol.* **1999**, *309*, 3.
- Li, L.; Darden, T. A.; Bartolotti, L.; Kominos, D.; Pedersen, L. G. *Biophys. J.* **1999**, *76*, 2871.
- Krebs, M. R. H.; Bromley, E. H. C.; Donald, A. M. *J. Struct. Biol.* **2005**, *149*, 30.
- Batista, R. M. F.; Costa, S. P. G.; Raposo, M. M. M. *Tetrahedron Lett.* **2004**, *45*, 2825.
- Cooper, J. H. *Lab. Invest.* **1974**, *31*, 232.
- Jin, L. W.; Claborn, K. A.; Kurimoto, M.; Geday, M. A.; Maezawa, I.; Sohraby, F.; Estrada, M.; Kaminsky, W.; Kahr, B. *Proc. Natl. Acad. Sci. U.S.A.* **2003**, *10*, 15294.
- Pauling, L.; Corey, R. B. *Proc. Natl. Acad. Sci. U.S.A.* **1951**, *37*, 729.
- Salemme, F. R. *Prog. Biophys. Mol. Biol.* **1983**, *42*, 95.
- Glennner, G. G.; Wong, C. W. *Biochem. Biophys. Res. Commun.* **1984**, *120*, 885.
- van Raaij, M. E.; Segers-Nolten, I. M.; Subramaniam, V. *Biophys. J.* **2006**, *91*, L96.

24. Hamer, F. M. *The Cyanine Dyes and Related Compounds*; Wiley: New York, 1964, Chapter IV pp. 32–73.
25. Hamer, F. M. *The Cyanine Dyes and Related Compounds*; Wiley: New York, 1964, Chapter VI, pp 148–192.
26. Dewar, M. J. S.; Zoebish, E. G.; Healy, E. F.; Stewart, J. J. P. *J. Am. Chem. Soc.* **1985**, *107*, 3902.
27. Pople, J. A.; Nesbet, R. K. *J. Chem. Phys.* **1954**, *22*, 571.